Lateral Distribution of a Pyrene-Labeled Phosphatidylcholine in Phosphatidylcholine Bilayers: Fluorescence Phase and Modulation Study†

R. C. Hresko, I. P. Sugár,‡ Y. Barenholz,§ and T. E. Thompson*
Department of Biochemistry, University of Virginia School of Medicine, Charlottesville, Virginia 22908
Received December 17, 1985; Revised Manuscript Received March 11, 1986

ABSTRACT: The lateral distribution of 1-palmitoyl-2-[10-(1-pyrenyl)decanoyl]phosphatidylcholine (PyrPC) was studied in small unilamellar vesicles of 1,2-dipalmitoyl-, 1,2-dimyristoyl-, and 1-palmitoyl-2-oleoylphosphatidylcholine (DPPC, DMPC, and POPC, respectively) under anaerobic conditions. The DPPC and DMPC experiments were carried out over temperature ranges above and below the matrix phospholipid phase transition temperature (T_m). The excimer to monomer fluorescence intensity ratio (E/M) was determined as a function of temperature for the three PyrPC/lipid mixtures. Phase and modulation data were used to determine the temperature dependence of pyrene fluorescence rate parameters in gel and in liquid-crystalline bilayers. These parameters were then used to (1) provide information about excited-state fluorescence in phospholipid bilayers, (2) calculate the concentration of the probe within liquid-crystalline and gel domains in the phase transition region of PyrPC in DPPC, and (3) simulate E/M vs. temperature curves for three systems whose phase diagrams are different. From the simulated curves we could determine the relationship between the shape of the three simulated E/M vs. temperature curves and the lateral distribution of the probe. This information was then used to interpret the three experimentally derived E/M vs. temperature curves. Our results indicate that PyrPC is randomly distributed in pure gel and fluid phosphatidylcholine bilayers. In the phase transition region, PyrPC molecules preferentially distribute in fluid phases in DPPC but distribute almost equally between fluid and gel phases in DMPC. There is, however, no gel-phase immiscibility in these systems.

In research on lipid bilayers and biological membranes so-called fluorescent probe molecules have very frequently been used to examine the molecular dynamics and the structural organization of natural membrane components. Two distinctly different types of probes have been employed. One type, exemplified by diphenylhexatriene, is a fluorescent lipid molecule that strongly partitions into the hydrophobic interior of the bilayer but is not in anyway genuinely related to the component phospholipid molecules. A probe of this type is essentially an impurity in the system whose properties give average information about its immediate surroundings in the bilayer. The second type of probe, exemplified by a phospholipid covalently labeled with a fluorescent fatty acid, is genuinely related more or less closely to the component phospholipid molecules of the bilayer or biological membrane. With this type of probe the objective of the study is to use the observable properties of the probe to draw conclusions about the dynamics and structure of an individual component phospholipid molecule. In this case it is hoped that the lipid probe will exactly mimic the properties of the unobservable component molecules of the bilayer. The key question to be answered about this type of probe is the following: how good a mimic is the probe?

Pyrene-labeled lipids have been used extensively to study the physical and structural properties of lipid membranes. Some of these studies include spontaneous interbilayer lipid transfer (Frank et al., 1983; Roseman & Thompson, 1980; Massey et al., 1984, 1982; Pownall et al., 1982), protein-mediated interbilayer lipid transfer (Wong et al., 1984), lateral diffusion (Galla et al., 1979), and phospholipid lateral phase separation (Somerharju et al., 1985; Wiener et al., 1985). All of the above studies are based upon the ability of pyrene to form excited-state dimers (excimers) between an excited-state monomer and a ground-state pyrene molecule (Kasper & Forster, 1955). The fluorescence emission of the excimer is at longer wavelengths relative to that of the excited monomer. Birks et al. (1963) used the following mechanism to illustrate the various kinetic process

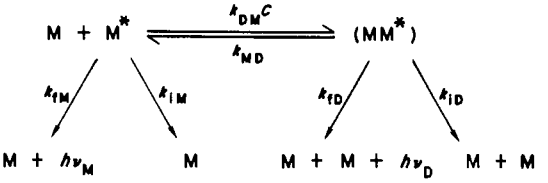

where M* and MM* are excited monomer and excimer molecules, k_{fM} and k_{fD} are the monomer and excimer fluorescence decay parameters, k_{iM} and k_{iD} are the monomer and excimer nonradiative decay parameters, $k_{DM}C$ is the rate constant for excimer formation, k_{DM} is the second-order rate constant for excimer formation, C is the probe concentration, and k_{MD} is the rate constant for the regeneration of excited monomer from the dissociation of excimer.

The fluorescence parameter most frequently measured in pyrene studies is the ratio of the excimer to monomer fluorescence intensity (E/M)

$$E/M = (k_{fD}/k_{fM})k_{DM}C(k_D + k_{MD})^{-1} \quad (1)$$

where k_D is the sum of the radiative and nonradiative excimer decay parameters ($k_{fD} + k_{iD}$) and $(k_D + k_{MD})^{-1}$ is the lifetime of the excimer.

Since pyrene-labeled lipids are widely used in lipid research, the objective of this study is to determine how well 1-palmitoyl-2-[10-(1-pyrenyl)decanoyl]phosphatidylcholine (PyrPC)[1]

† Supported by NIH Grants GM-14628 and HL 17576, NIH Training Grant GM-07294, and BSF 2772.
‡ Visiting Assistant Professor from the Institute of Biophysics, Semmelweis Medical University, Budapest 1444, Hungary.
§ Also affiliated with the Department of Biochemistry, The Hebrew University, Hadassah Medical School, Jerusalem, Israel.

0006-2960/86/0425-3813$01.50/0

can mimic the physical properties of nonfluorescent phosphatidylcholines in the bilayer. In order to answer this question, we have determined the lateral distribution of PyrPC in three different phosphatidylcholine matrices (POPC, DPPC, and DMPC) by fluorescence methods. Since pyrene is highly quenched by oxygen, all fluorescence experiments were done under anaerobic conditions. The DPPC and DMPC experiments were carried out over a temperature range above and below the matrix lipid phase transition temperature (T_m).

The lateral distribution of the probe is directly related to the local probe concentration. In randomly mixed systems the local probe concentration is equal to the total probe concentration, but in phase-separated systems the local probe concentration and the total probe concentration will differ. The local probe concentration is very difficult to determine experimentally and therefore techniques for examining phase separation tend to be indirect and semiquantitative.

E/M is proportional to the local probe concentration (see eq 1), and therefore, an abrupt increase in E/M observed upon cooling a system from above to below the matrix lipid T_m has been attributed to a change in the local probe concentration (Galla & Sackmann, 1975, 1974; Freire et al., 1983; Correa-Freire et al., 1982; Somerharju et al., 1985; Usher et al., 1978). However, E/M is related to other rate parameters as well, and therefore, changes in these parameters with temperature may also affect the E/M ratio in this temperature range.

In this study we measure the temperature dependence of the E/M ratio for a liquid-crystalline system (PyrPC in POPC) and for two systems that undergo a phase change over the temperature range studied (PyrPC in DPPC and PyrPC in DMPC). We then determine the temperature dependence of the pyrene fluorescence rate parameters (k_{fD}/k_{fM}), $k_{DM}C$, k_{MD}, k_D, and k_M using steady-state and phase/modulation fluorometry. k_M is the sum of the radiative and nonradiative monomer decay parameters ($k_{fM} + k_{iM}$). The rate parameters are then used to (1) provide information about excited-state reactions in phospholipid bilayers, (2) simulate E/M vs. temperature curves for systems whose lateral distribution is known in order to interpret the three experimentally derived E/M vs. temperature curves, and (3) compute the concentration of the probe in liquid-crystalline (C_f) and gel (C_g) domains in the phase transition region of the PyrPC/DPPC mixture.

Our results indicate that, in small unilamellar vesicles, PyrPC is randomly distributed in gel and liquid-crystalline phosphatidylcholine bilayers. In the phase transition region, PyrPC molecules preferentially distribute in fluid phases in DPPC but distribute almost equally between fluid and gel phases in DMPC. There is, however, no immiscibility in the gel phase in these systems.

Materials and Methods

Materials. 1,2-Dipalmitoyl-, 1,2-dimyristoyl-, 1-palmitoyl-2-oleoyl-, and monopalmitoylphosphatidylcholines (DPPC, DMPC, POPC, and lysoPC, respectively) were purchased from Avanti Biochemical, Inc. The lipids were checked for purity by thin-layer chromatography (TLC) and then stored at −20 °C under nitrogen. 10-(1-pyrenyl)decanoic acid was purchased from Molecular Probes Inc. and then repurified by high-performance liquid chromatography (HPLC) (Hresko et al., 1985). We have previously demonstrated that pyrene fatty acids that are purified commerically or in the laboratory by silica column chromatography and analyzed by TLC contain fluorescent impurities. Calorimetric scans of purified PyrPC multilamellar vesicles (MLVs) show a single relatively sharp peak (data not shown) while the scans of PyrPC MLVs whose fatty acids were not purified by HPLC have a shoulder at the low-temperature side which suggests that the nonpurified sample is not as pure (Somerharju et al., 1985; our unpublished results).

1-Palmitoyl-2-[10-(1-pyrenyl)decanoyl]phosphatidylcholine was synthesized by using the method of Mason et al. (1981). LysoPC was reacylated with 10-(1-pyrenyl)decanoic acid by using the catalyst 4-pyrrolidinopyridine. The product was then purified by thin-layer chromatography.

Preparation of Liposomes. All fluorescent experiments were carried out with small unilamellar vesicles (SUVs). SUVs were prepared by cosonicating the pyrene/lipid mixtures in 10 mM Pipes, 1 mM EDTA, and 0.02% NaN_3, pH 7.4, buffer under nitrogen by using the procedure of Barenholz (1977). Large liposomes were separated from the small vesicles by differential ultracentrifugation. SUVs were stored overnight under nitrogen above the matrix lipid phase transition temperature. Prior to fluorescent measurements, the vesicle solutions were flushed with nitrogen for 60 min above the matrix lipid T_m in gas-tight cuvettes.

Fluorescence Measurements. All measurements were performed on an SLM 4800 spectrofluorometer (SLM-Aminco, Urbana, IL). The polarizers were removed to improve signal intensity. The sample cuvette was stirred continuously and temperature regulated to ±0.1 °C. All samples were incubated at the desired temperature for at least 20 min prior to the actual measurement. The PyrPC concentration was kept low, 8.9×10^{-6} M, to minimize the absorption at 378 nm which was negligible under these conditions. The inner filter effects reduce the monomer and excimer intensities to the same degree and therefore cancel out in the E/M ratio.

Lifetime Measurements. The excitation was 346 nm (1-nm slit width), and the monomer and excimer emissions were 378 and 500 nm, respectively (16-nm slit width); 500 nm was selected to eliminate the contribution of the monomer to excimer fluorescence. Phase and modulation values were determined at 6-MHz modulation frequency relative to a POPOP reference solution (Lakowicz et al., 1981). Each value is an average of at least 300 measurements. The probe/lipid concentration range at which the pyrene rate parameters were calculated was between 7 and 12 mol %. At lower mole ratios measured phase angles are greater than 70°, and the calculated rate parameters become very sensitive to small errors in the measured phase angles. Each PyrPC/phosphatidylcholine system was studied at three to five different concentrations of probe/lipid. The rate parameters reported in this paper are averages of the values obtained at the different concentrations. All parameters were concentration independent except E/M and $k_{DM}C$. E/M and $k_{DM}C$ values for a 10% probe/lipid ratio were determined from plots of these parameters as a function of probe/lipid concentration.

The pyrene rate parameters $k_{DM}C$, k_{MD}, k_D, and k_M were determined from phase and modulation data by using either

[1] Abbreviations: C_{16}SPM, *N*-palmitoylsphingomyelin; C_{18}SPM, *N*-stearoylsphingomyelin; DEPC, dielaidoylphosphatidylcholine; DMPC, dimyristoylphosphatidylcholine; DPPC, dipalmitoylphosphatidylcholine; HPLC, high-performance liquid chromatography; LysoPC, monopalmitoylphosphatidylcholine; MLVs, multilamellar vesicles; POPC, 1-palmitoyl-2-oleoylphosphatidylcholine; PyrPC, 1-palmitoyl-2-[10-(1-pyrenyl)decanoyl]phosphatidylcholine; PyrSPM, *N*-[10-(1-pyrenyl)decanoyl]sphingomyelin; SUVs, small unilamellar vesicles; TLC; thin-layer chromatography; T_m, phase transition temperature; τ_D, lifetime of excimer fluorescence; EDTA, ethylenediaminetetraacetic acid; Pipes, 1,4-piperazinediethanesulfonic acid; POPOP, 1,4-bis(5-phenyl-2-oxazolyl)-benzene.

a closed form or an iterative analysis which are both described in detail in Appendix I. The close form method is a modification of the original method of Birks et al. (1963).

The two methods described above are valid for single phase systems only. In the phase transition region where gel and fluid domains coexist, both analyses fail because there are two sets of rate parameters corresponding to each type of domain, k_{DM}^g, k_{MD}^g, k_D^g, k_M^g, $(k_{fD}/k_{fM})^g$ and k_{DM}^f, k_{MD}^f, k_D^f, k_M^f, $(k_{fD}/k_{fM})^f$. Since it is possible to determine the temperature dependence of the pyrene rate parameters in pure gel and liquid-crystalline phases, the two sets of rate parameters in the mixed phase region were estimated by extrapolating these functions from the pure phases. k_{DM} values were obtained by dividing $k_{DM}C$ by the probe/total lipid ratio. It is assumed that the probe is randomly distributed outside of the phase transition region for reasons stated under Discussion. The probe concentration in fluid (C_f) and gel (C_g) domains were determined by solving the following two nonlinear implicit equations which are derived in Appendix I.

$$E/M = \left[(1 - \sigma_M)\frac{k_{DM}^g C_g k_{fD}^g}{\lambda_1^g \lambda_2^g k_{fM}} + \sigma_M \frac{k_{DM}^f C_f k_{fD}^f}{\lambda_1^f \lambda_2^f k_{fM}} \right] \Big/ [g_1/\lambda_1^g + g_2/\lambda_2^g + \delta_1/\lambda_1^f + \delta_2/\lambda_2^f] \quad (2)$$

$$\phi_M = \tan^{-1}\left[\omega \left[\frac{g_1}{(\lambda_1^g)^2 + \omega^2} + \frac{g_2}{(\lambda_2^g)^2 + \omega^2} + \frac{\delta_1}{(\lambda_1^f)^2 + \omega^2} + \frac{\delta_2}{(\lambda_2^f)^2 + \omega^2} \right] \Big/ \left[\frac{g_1\lambda_1^g}{(\lambda_1^g)^2 + \omega^2} + \frac{g_2\lambda_2^g}{(\lambda_2^g)^2 + \omega^2} + \frac{\delta_1\lambda_1^f}{(\lambda_1^f)^2 + \omega^2} + \frac{\delta_2\lambda_2^f}{(\lambda_2^f)^2 + \omega^2} \right] \right] \quad (3)$$

where

$$\sigma_M = C_f \frac{C_T - C_g}{C_f - C_g} \frac{1}{C_T}$$

C_T = total probe/lipid ratio

$$X = k_M + k_{DM}C \qquad Y = k_D + k_{MD}$$

$$\lambda_{1,2} = (1/2)[X + Y \mp \{(Y - X)^2 + 4k_{DM}k_{MD}C\}^{1/2}]$$

$$g_1 = (1 - \sigma_M)\left(\frac{\lambda_2^g - X^g}{\lambda_2^g - \lambda_1^g}\right) \qquad \delta_1 = \sigma_M\left(\frac{\lambda_2^f - X^f}{\lambda_2^f - \lambda_1^f}\right)$$

$$g_2 = (1 - \sigma_M)\left(\frac{X^g - \lambda_1^g}{\lambda_2^g - \lambda_1^g}\right) \qquad \delta_2 = \sigma_M\left(\frac{X^f - \lambda_1^f}{\lambda_2^f - \lambda_1^f}\right)$$

The two equations were solved by using a two-dimensional grid search to a precision of 1 part in 32000.

The excimer lifetime (τ_D) can be calculated from both phase and modulation data (Lakowicz & Balter, 1982)

$$\tau_D = (1/\omega) \tan (\phi_D - \phi_M) \quad (4)$$

$$\tau_D = (1/\omega)[(m_M/m_D)^2 - 1]^{1/2} \quad (5)$$

where ω is the angular frequency of the modulation, ϕ_M and ϕ_D are the monomer and excimer phase shifts, respectively, and m_M and m_D are the monomer and excimer demodulation ratios, respectively. It is important to note that it is the eximer phase shift or demodulation factor "relative" to the respective monomer value that is directly proportional to the excimer lifetime. This relationship stems from the fact that excimers are not excited directly but are formed by excited monomers. Modulation lifetimes (eq 5) were used exclusively because phase lifetimes are sensitive to small errors in the measured phase angles at longer lifetimes (Spencer, 1970).

Steady-State Measurements. Emission scans were taken immediately following the lifetime measurements. The sample intensity was recorded relative to a triangular cuvette containing a reference solution of rhodamine B (3 g/L in ethylene glycol). The samples were excited at 346 nm (2-nm slit width), and the emission was scanned from 360 to 600 nm (2-nm slit width) in increments of 1 nm. Each datum point was an average of 10 measurements. The ratio of the excimer to monomer intensities was determined in the following manner. All spectra were corrected for Raman and light-scattering effects by subtracting the emission spectrum of an unlabeled, but otherwise identical, vesicle solution measured under the same experimental conditions. The spectra were then normalized to the first monomer intensity peak. A pure monomer spectrum was obtained by measuring the emission of a very dilute PyrPC/lipid mixture (0.0084 mol %). The probability of finding two probe molecules in a single vesicle was negligible. The excimer spectrum at a particular concentration was obtained simply by subtracting the monomer spectrum from the total emission spectrum. The excimer to monomer ratios reported in this paper are based on integrated areas unless noted otherwise. The integration was performed by using a program supplied by SLM. It is important to note that since reliable correction factors could not be obtained over the entire range of emission, the spectra were not corrected for the wavelength dependence of the photomultiplier tubes.

RESULTS

The lateral distribution of PyrPC was studied as a function of temperature in three different phosphatidylcholine matrices (POPC, DPPC, and DMPC). Small unilamellar vesicles were used in all experiments unless noted otherwise. Since the phase transition temperatures of PyrPC and POPC are 15 (Somerharju et al., 1985) and −5 °C (Silvius, 1982), respectively, PyrPC/POPC liposomes were in the liquid-crystalline phase in the temperature range examined, 25–50 °C. The DPPC and DMPC experiments were carried out over a temperature range above and below the respective matrix phospholipid phase transition temperatures of 41 and 23 °C (Silvius, 1982).

Temperature Dependence of Fluorescence Parameters. E/M vs. temperature plots of PyrPC/POPC, PyrPC/DPPC, and PyrPC/DMPC mixtures are depicted in Figure 1A. E/M increases almost linearly with temperature for the PyrPC/POPC mixture and for the PyrPC/DPPC and PyrPC/DMPC mixtures above their respective matrix T_m's. The PyrPC/DPPC plot is N-shaped with a minimum at 40 °C and a maximum between 30 and 35 °C. In contrast to the DPPC curve, the DMPC plot has only a small break at 15 °C instead of a peak.

It is assumed that the reaction scheme shown in the introduction is valid in fluid and in gel phases. Although we realize that pyrene fluorescence in lipid bilayers may be described by more complex models, we are prevented from applying these models by the limited number of reliable experimental observables. In the future it may be possible to explore more complex reaction schemes by using multifrequency phase and modulation fluorometry. It is important to note, however, that the pyrene absorption spectrum is the same above and below the matrix lipid T_m (data not shown) which indicates that

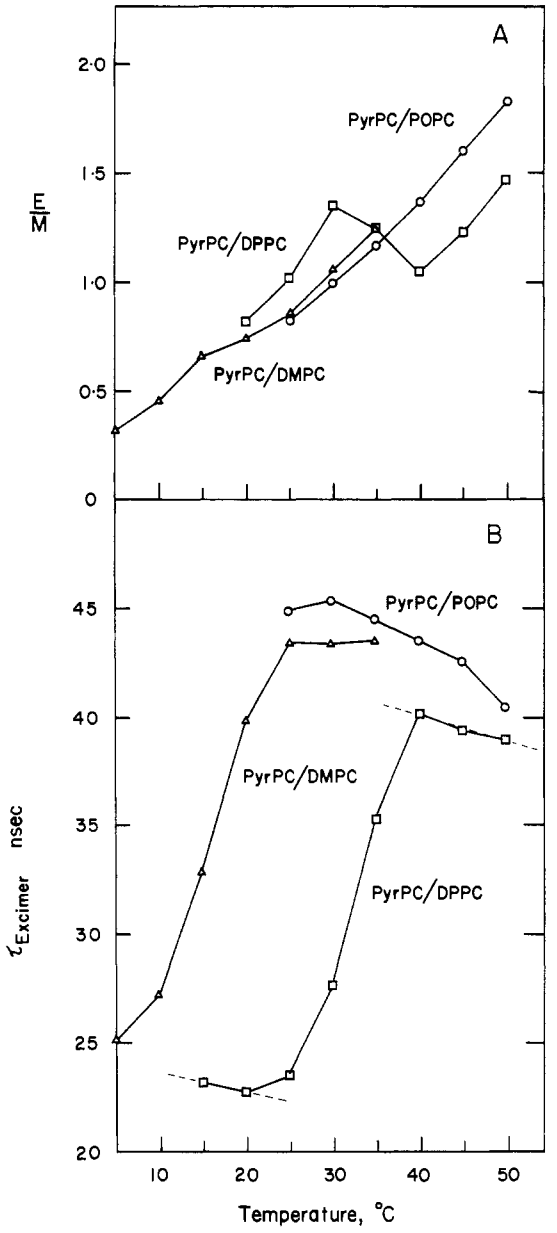

FIGURE 1: (A) Temperature dependence of the E/M ratio for (10:90) PyrPC/POPC (○), (10:90) PyrPC/DPPC (□), and (10:90) PyrPC/DMPC (△) small unilamellar vesicles. The E/M ratio is the integrated intensity of excimer fluorescence relative to the integrated intensity of monomer fluorescence. For details, see Materials and Methods. (B) Excimer lifetime as a function of temperature for the three PyrPC/PC mixtures described above. Modulation values were used to calculate the lifetimes as described under Materials and Methods. Dashed lines represent the temperature dependence of the excimer lifetime in fluid and in gel phases for PyrPC in DPPC.

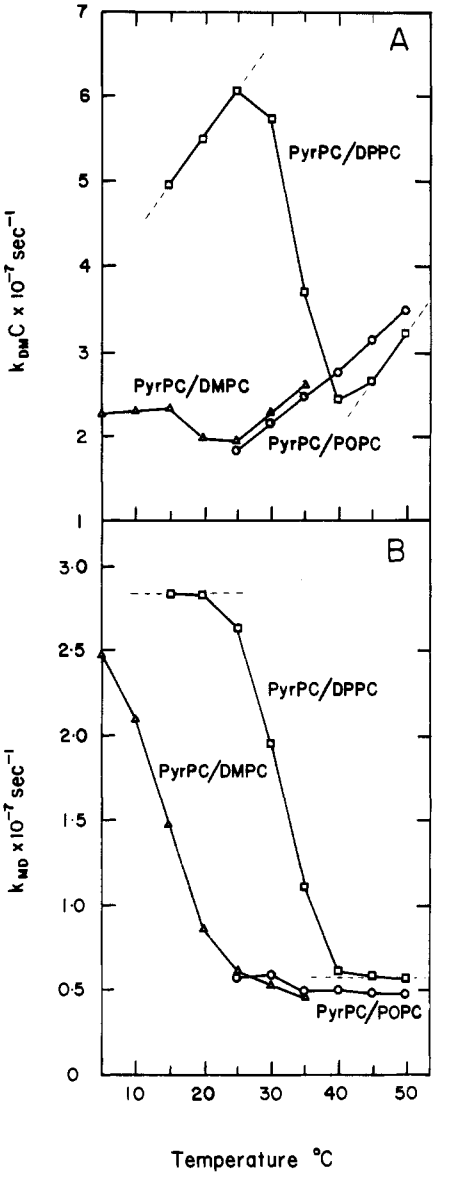

FIGURE 2: (A) Rate of excimer formation ($k_{DM}C$) as a function of temperature for (10:90) PyrPC/POPC (○), (10:90) PyrPC/DPPC (□), and (10:90) PyrPC/DMPC (△) SUVs. (B) Rate of excimer dissociation (k_{MD}) as a function of temperature for the three PyrPC/PC mixtures. Dashed lines represent the temperature dependence of $k_{DM}C$ or k_{MD} in fluid and in gel phases for PyrPC in DPPC.

excimer formation is an excited-state process.

E/M is directly related to the lifetime of the excimer, τ_D (see eq 1). τ_D decreases with increasing temperature for PyrPC in POPC (Figure 1B). The two dashed lines in the PyrPC/DPPC plot indicate that τ_D decreases slightly with increasing temperature in gel and in fluid phases. The excimer lifetime in the gel state is approximately 2-fold shorter than in the liquid-crystalline state. The reported τ_D values in the phase transition region are intensity weighted averages of the two phases. It is apparent that the temperature points that delimit the phase transition of PyrPC in DMPC are not as well-defined as in the PyrPC/DPPC system; nevertheless, τ_D is also about 2-fold shorter in the gel phase relative to the lifetime in the fluid phase.

Temperature Dependence of Rate Parameters. E/M vs. temperature plots can provide important information on the lateral distribution of the probe if the relationship between shape and lateral organization is known. E/M depends on several pyrene fluorescence rate parameters for both single-phase and mixed-phase systems (see eq 1 and 2). The first step in determining the lateral distribution of PyrPC is to determine the temperature dependence of the pyrene rate parameters $k_{DM}C$, k_D, k_{MD}, k_M, and k_{fD}/k_{fM} for the three lipid mixtures. In the phase transition region of PyrPC/DPPC and PyrPC/DMPC mixtures, applications of eq 10–15 give apparent rate parameters. Since in the mixed-phase region there is one set of parameters corresponding to the liquid-crystalline phase and another for the gel phase, each apparent rate parameter calculated in this region is a complex average of the two rate parameters for the two domains.

$k_{DM}C$ vs. temperature plots are shown in Figure 2A. Similar to the E/M result, the rate of excimer formation,

$k_{DM}C$, increases linearly with increasing temperature for PyrPC in POPC. The two dashed lines in the PyrPC/DPPC plot indicate the temperature dependence of $k_{DM}C$ in pure liquid-crystalline and gel phases. If the two lines are extended into the phase transition region, $k_{DM}C$ is more than 6-fold higher in the gel than in the liquid-crystalline phase. The same trend is observed in the PyrPC/DMPC plot; however, the difference in $k_{DM}C$ between the two phases is less than 2-fold.

The excimer lifetime is inversely proportional to the sum of the three rate parameters k_{fD}, k_{iD}, and k_{MD} (Lakowicz & Balter, 1982). Plots of the temperature dependence of k_{MD}, the rate of excimer dissociation, for all three lipid mixtures are presented in Figure 2B. Under liquid-crystalline conditions, k_{MD} decreases slightly with increasing temperature for all three systems, and the absolute magnitude is approximately the same. k_{MD} in the gel phase is at least 5-fold higher than in the fluid phase for both PyrPC/DPPC and PyrPC/DMPC mixtures. k_{fD} and k_{iD} are combined into a single rate parameter k_D because it is difficult to separate experimentally k_{fD} and k_{iD}. In plots of k_D vs. temperature plots shown in Figure 3A, k_D increases with increasing temperature for all three lipid systems.

An estimate of the inverse of the monomer lifetime at infinite dilution gives k_M which increases with temperature in fluid bilayers of POPC, DPPC, and DMPC (Figure 3B). However, in the gel state of DPPC and DMPC, k_M is temperature independent and greater in magnitude than in the fluid phase.

The ratio of the excimer to monomer fluorescence decay parameters (k_{fD}/k_{fM}) was calculated from E/M, $k_{DM}C$, and τ_D data. The results are shown in Figure 3C. k_{fD}/k_{fM} increases with increasing temperature for PyrPC in POPC and PyrPC in DMPC. The two dashed lines in the PyrPC/DPPC plot indicate k_{fD}/k_{fM} values in gel and in fluid phases.

Discussion

The objective of this study is to determine how well PyrPC mimics the physical properties of naturally occurring phosphatidylcholines in bilayers. In order to answer this question, we have examined the lateral organization of PyrPC in three different phosphatidylcholine bilayers using steady-state and dynamic fluorescence techniques.

The simplest system, PyrPC in POPC, is liquid crystalline throughout the observed temperature region. It is generally assumed that pyrene probes above their T_m are randomly distributed in a fluid bilayer (Galla & Sackmann, 1974; Vanderkooi & Callis, 1974). An oxygen-quenching study indicates that this particular system is in fact randomly mixed above 15 °C (Chong & Thompson, 1985). The other two systems, PyrPC in DPPC and PyrPC in DMPC, both undergo a phase transition in the observed temperature range. The following information indicates that these two systems are randomly mixed outside their respective phase transition regions: (1) the shape of the E/M vs. temperature plots above their respective matrix phospholipid T_m are similar to the PyrPC/POPC curve; (2) E/M vs. temperature simulations, which are discussed later, also suggest a random probe distribution outside of the phase transition range; (3) the phase diagram of PyrPC in DPPC obtained from calorimetric studies on multilamellar vesicles indicates that, at a lipid composition of 10% probe, PyrPC and DPPC molecules are randomly mixed in the pure gel phase (Somerharju et al., 1985; our unpublished results); (4) a spontaneous phospholipid transfer experiment on PyrPC in DMPC suggests that PyrPC in randomly distributed above the DMPC T_m (Roseman & Thompson, 1980).

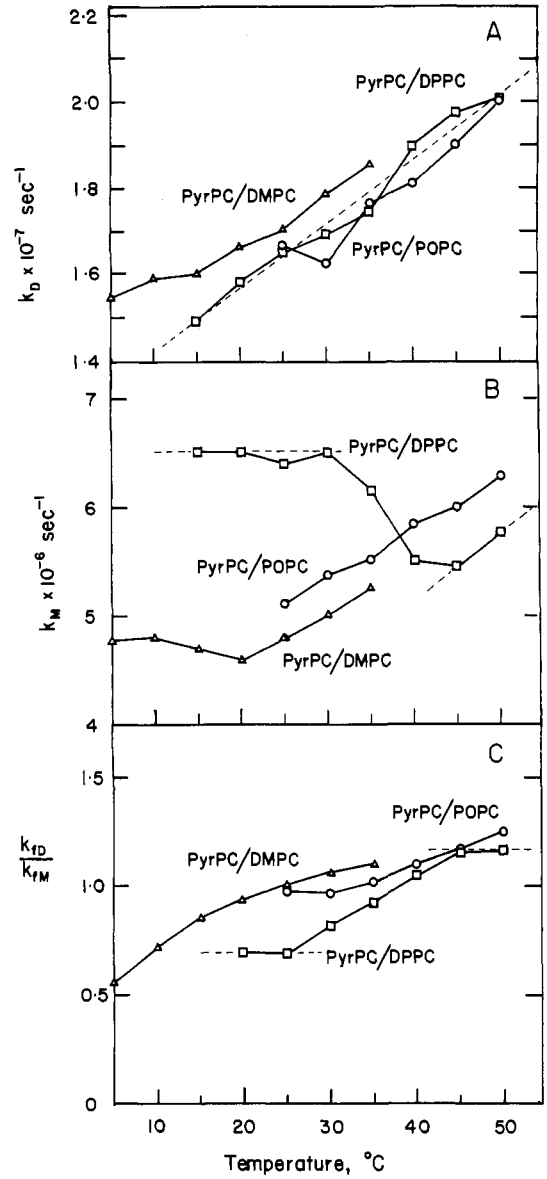

FIGURE 3: (A) Temperature dependence of k_D for (10:90) PyrPC/POPC (○), (10:90) PyrPC/DPPC (□), and (10:90) PyrPC/DMPC (△) SUVs. k_D is the sum of the excimer radiative and nonradiative decay parameters. (B) Temperature dependence of k_M for the same three PyrPC/PC mixtures. k_M is the sum of the monomer radiative and nonradiative decay parameters. (C) Temperature dependence of the excimer to monomer fluorescence decay parameters (k_{fD}/k_{fM}) for the three PyrPC/PC mixtures. Dashed lines represent the temperature dependence of k_D, k_M, or k_{fD}/k_{fM} in fluid and in gel phases for PyrPC in DPPC.

The results discussed earlier indicate that PyrPC is randomly mixed in fluid and in gel bilayers of DPPC and DMPC. However, there is little known about the distribution of PyrPC in the phase transition regions of DPPC and DMPC where both fluid and gel phases coexist. The most common method used to examine the lateral distribution of the probe in the phase transition region of the matrix phospholipid is to determine the temperature dependence of the E/M ratio. The E/M ratio increases almost linearly with increasing temperature for PyrPC in POPC from 25 to 50 °C and for the PyrPC/DPPC and PyrPC/DMPC mixtures above their respective matrix lipid T_m's (Figure 1A). If excimer formation is diffusion controlled in liquid-crystalline bilayers, then the E/M ratio should increase with increasing temperature. As the temperature is lowered from above to below the DPPC T_m, the E/M ratio increases in the PyrPC/DPPC plot. This

anomalous behavior is thought to indicate a lateral redistribution of the probe. As DPPC gel domains form upon lowering the temperature below the T_m, PyrPC molecules concentrate in the fluid phase resulting in an increased E/M (Galla & Sackmann, 1974, 1975; Correa-Freire et al., 1982; Freire et al., 1983; Somerharju et al., 1985; Usher et al., 1978). Although a change in the local pyrene concentration is the most reasonable explanation for the sharp increase in E/M below the DPPC T_m, E/M is related to other rate parameters as well, and changes in these parameters with temperature may also affect the E/M ratio in this temperature range. Also it is unclear from an E/M vs. temperature plot whether the probe is randomly mixed or phase separated in the pure gel state. The E/M vs. temperature plot for PyrPC in DMPC is very different from the PyrPC/DPPC plot. The discontinuity in the curve below the DMPC T_m is in sharp contrast to the peak seen below the DPPC T_m. It is not apparent from the shape of the PyrPC/DMPC plot what the lateral distribution of the probe is. Since there are limitations in understanding the lateral organization of the probe from an E/M vs. temperature plot alone, it was decided to determine first the temperature dependence of the pyrene fluorescence rate parameters and then use these parameters to simulate E/M vs. temperature curves for systems of known lateral distribution. The simulated curves are then compared with the experimental curves.

The pyrene fluorescence rate parameters themselves can provide information about excited-state reactions in phospholipid bilayers. However, since this aspect is a secondary topic not directly related to the overall study, it is discussed in Appendix II.

Simulations of Temperature Dependence of E/M. E/M vs. temperature curves were simulated for 5%, 10%, and 20% PyrPC/DPPC mixtures by using eq 2. Since the shape of the simulated curves are independent of probe concentration, only the curves for 10% PyrPC in 90% DPPC are presented. The gel and liquid-crystalline rate parameters that were calculated for PyrPC in DPPC from phase/modulation and steady-state data were used. The two dashed lines seen in Figures 2 and 3 indicate the temperature dependence of the rate parameters in the pure phases. It is assumed that above the DPPC T_m (41 °C) the system is liquid crystalline and below 25 °C it is gel. The temperatures 41 and 25 °C were chosen because the rate parameters $k_{DM}C$ and k_{MD} both changed dramatically at approximately these temperatures. In the temperature region where gel and liquid-crystalline domains coexist, the two sets of rate parameters corresponding to each domain were estimated by extrapolating the two dashed lines. C_f and C_g values were estimated from the liquidus and solidus lines in three different hypothetical PyrPC/DPPC phase diagrams. In the first type, the hypothetical PyrPC/DPPC system is nearly ideal (Figure 4A). In the second type the system is more nonideal, but there is no gel-phase immiscibility (Figure 4B). The phase diagrams depicted in Figure 4A,B are based on the previously reported diagrams obtained from calorimetric studies on multilamellar vesicles [DMPC–DPPC (Mabrey & Sturtevant, 1976); PyrPC–DPPC (Somerharju et al., 1985)]. The phase diagram for the third hypothetical system is peritectic (Figure 4C). It is assumed that the two sets of pyrene fluorescence rate parameters for the two immiscible gel phases, g_1 and g_2, are both equal to the experimentally determined gel rate parameters for PyrPC in DPPC. For excellent reviews on phase diagrams, see Lee (1977) and Sugár and Monticelli (1985).

The simulated E/M vs. temperature curve for the PyrPC/DPPC system which is nearly ideal is depicted in Figure 5A. There is an increase in E/M with increasing temperature in the fluid phase, and upon lowering the temperature through the phase transition region, there is a small E/M maximum followed by an abrupt decrease in E/M. The gel-phase slope is lower than the fluid-phase slope. Figure 5A is very similar to the experimentally derived E/M vs. temperature curve for 10% PyrPC in 90% DMPC (Figure 5D).

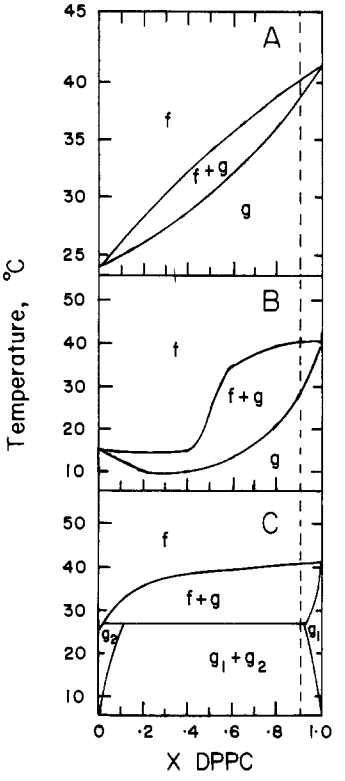

FIGURE 4: Phase diagrams for three hypothetical PyrPC/DPPC mixtures. The dashed line depicts the lipid composition at which the fluorescence experiments were carried out (10:90, PyrPC/DPPC). f is the fluid phase, g is the gel phase, and f+g is the mixed phase. Panel A is a phase diagram for a PyrPC/DPPC system with nearly ideal mixing. Panel B is a phase diagram for a PyrPC/DPPC system which is completely miscible, but the mixing is more nonideal. Panel C is a peritectic PyrPC/DPPC phase diagram. g_1 and g_2 are the two immiscible gel phases.

Figure 5B is the simulated E/M vs. temperature curve for the PyrPC/DPPC system which is nonideal but which is not immiscible in the gel phase. There is an abrupt increase in E/M upon lowering the temperature below the matrix phospholipid T_m followed by a decrease in E/M at lower temperatures. Since it is assumed that the probe is completely miscible in pure gel and fluid phases, this curve is identical with Figure 5A outside the mixed-phase region. Figure 5B closely resembles the experimentally derived E/M vs. temperature curve for 10% PyrPC in 90% DPPC (Figure 5E). Both curves have an E/M maximum in the phase transition region at approximately 37.5 °C. The slope in the gel-phase region is less than that in the fluid phase in both curves. This result is not unexpected since the simulated curve was based upon calorimetric studies of PyrPC in DPPC; however, it is an important check of our analysis and also provides information regarding the distribution of the probe in the phase transition region of DPPC. The experimental E/M vs. temperature plots (Figure 5D,E) are obtained by using multilamellar vesicles. MLV results are presented because two of the hypothetical phase diagrams are based on MLV experiments.

The simulated E/M vs. temperature curve for PyrPC in DPPC which assumes immiscibility in the gel phase is shown

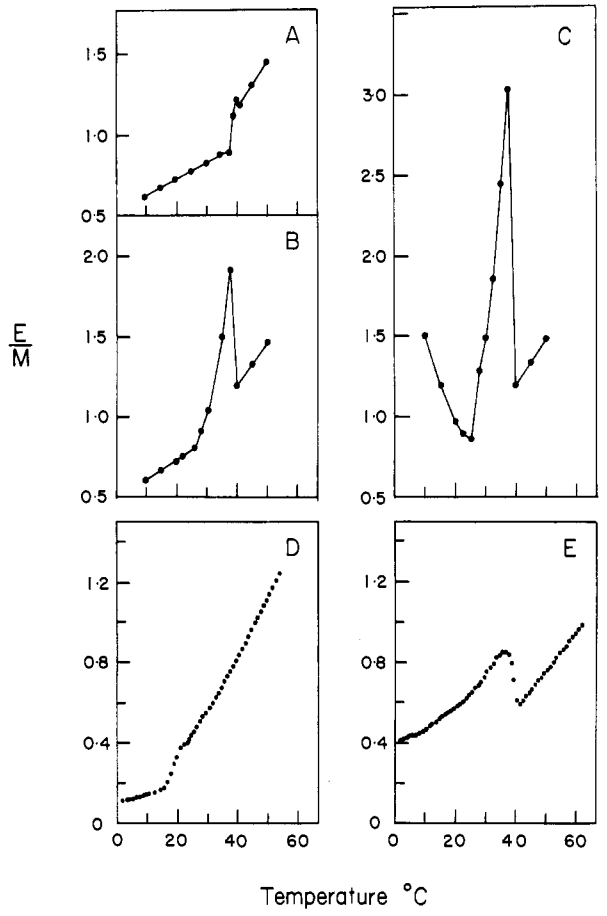

FIGURE 5: (A–C) Simulated E/M vs. temperature curves for the three hypothetical PyrPC/DPPC systems. The method used to simulate the plots is described under Discussion. (A) Simulation for a (10:90) PyrPC/DPPC system with nearly ideal mixing. (B) Simulation for a (10:90) PyrPC/DPPC system with complete miscibility, but the mixing is more nonideal. (C) Simulation for a peritectic (10:90) PyrPC/DPPC system. (D and E) Experimental E/M vs. temperature scans for (D) (10:90) PyrPC/DMPC and (E) (10:90) PyrPC/DPPC multilamellar vesicles. MLVs were prepared by vortexing the dried lipid mixture in 10 mM Pipes, 1 mM EDTA, and 0.02% NaN_3, pH 7.4, buffer above the matrix lipid T_m. Samples were flushed with nitrogen for 1 h and then excited at 346 nm, and the emission was monitored at 378 and 470 nm on two monochromators. The ratio of the intensities at 470 nm/378 nm (E/M) and the sample temperature were interfaced directly to a Hewlett-Packard 9825A computer. Each data point is an average of 100 E/M values. The temperature was scanned at a rate of 30 °C/h. No corrections were made for light scattering which was negligible at the lipid concentration of 0.11 mM.

in Figure 5C. Since the probe is assumed to be completely miscible in the fluid phase, this curve is identical with Figure 5A,B above the DPPC T_m. An E/M peak is seen in the phase transition region that is larger than that observed in Figure 5B. In contrast to the results obtained for the miscible systems, E/M decreases with increasing temperature in the mixed gel state. It is important to note that since we have never experimentally observed E/M to decrease with increasing temperature in the gel state, our original assumption that PyrPC is randomly mixed in DPPC and DMPC gel phases is probably correct.

The PyrPC in POPC curve (Figure 1A) closely resembles the simulated E/M vs. temperature curves above the matrix lipid T_m. Since it is assumed in the simulations that the probe is randomly distributed in the fluid matrix, PyrPC is probably randomly mixed in POPC.

E/M vs. temperature plots of 10% PyrPC in DMPC should in principle be simulated by using the rate parameters determined from phase and modulation data for 10% PyrPC in DMPC. However, the rate parameters determined for PyrPC in DMPC were not as reliable as those for PyrPC in DPPC. The rate parameters k_{MD} and k_{fD}/k_{fM} for PyrPC in DMPC never level off in the gel state as was observed for PyrPC in DPPC. The error in determining the PyrPC/DMPC rate parameters may be due to the low E/M ratio in the PyrPC/DMPC gel state. Since the fluorescence emission was observed with a 16-nm band-pass slit, a fraction of the monomer emission may contaminate the excimer signal at 500 nm due to the overlap of the monomer and excimer fluorescence bands. Fluorescence heterogeneity, which would be more pronounced at low E/M ratios, would effect the rate parameter determination (Birks et al., 1964). Nevertheless, the absolute values of the PyrPC/DPPC and the PyrPC/DMPC rate parameters above and below the matrix phospholipid T_m are very similar except for k_{DM}^g. k_{DM}^g values for PyrPC in DPPC are much larger than those calculated for PyrPC in DMPC. Therefore, we decided to repeat the simulations but with k_{DM}^g values similar to the PyrPC/DMPC case to see if the difference in the k_{DM}^g values changed the shape of the simulated E/M vs. temperature curves. The results show some minor differences (data not shown), but overall the shape of the three simulated E/M vs. temperature curves based on k_{DM}^g values similar to the PyrPC/DMPC case are very similar to the original simulations based on the k_{DM}^g values for PyrPC in DPPC.

Table I: Probe Concentration within Fluid and Gel Domains in the Phase Transition Region of 10% PyrPC in 90% DPPC

temp (°C)	E/M	ϕ_M	C_f	C_g
40	1.041	55.30	0.107	0.077
35	1.240	49.60	0.251	0.031
30	1.344	47.25	0.509	0.024
25	1.013	50.61	0.850	0.026

Since the difference in the pyrene rate parameters between the PyrPC/DPPC and PyrPC/DMPC mixtures has only a minor effect on the shape of the E/M vs. temperature curves, the difference in the phase transition region in the E/M vs. temperature plots for PyrPC in DPPC and PyrPC in DMPC is mainly due to a difference in the distribution of the probe. The discontinuity in the E/M vs. temperature plot for PyrPC in DMPC indicates that PyrPC distributes almost equally between fluid and gel domains of DMPC. In contrast there is a maximum in E/M if the probe preferentially distributes in the fluid domains such as is the case for PyrPC in DPPC. The height of the E/M peak is dependent upon the preference of the probe for the fluid state; the greater the preference, the larger the peak height. The difference in the lateral distribution of the probe in DPPC and DMPC bilayers may be attributed to the difference in chain length between DPPC and DMPC. DMPC molecules are shorter than the probe by approximately two methylene groups, and therefore, the pyrene moiety must be located more toward the center of the bilayer than it is in DPPC bilayers. Since the center of the bilayer is known to be the most fluid region of the bilayer (Seelig & Seelig, 1974; Hubbell & McConnell, 1971), DMPC bilayers may be able to accommodate the bulky pyrene moiety to a greater extent.

Determination of C_f and C_g. E/M vs. temperature curves provide a qualitative method for determining the lateral distribution of a pyrene-labeled probe. In this paper we have developed a fluorescent method described in detail under Materials and Methods and Appendix I for determining the concentration of the probe within fluid (C_f) and gel (C_g) domains in the phase transition region. The results, shown in

Table I for PyrPC in DPPC, indicate that as the temperature is decreased from 40 to 25 °C, C_f increases 8-fold while C_g remains essentially constant. This result indicates that PyrPC molecules preferentially distribute in fluid domains in the phase transition region of PyrPC in DPPC which supports the E/M vs. temperature simulations. By means of this method one can construct part of a phase diagram (see Table I) in spite of the fact that fluorescence measurements were carried out at only a single PyrPC/DPPC concentration. We note that there are relatively few methods for the determination of the real phase lines. In most cases one can determine only the onset and completion curves of the phase transition (McElhaney, 1982), which differ significantly from the solidus and liquidus curves, especially at the pure component extremes. Nevertheless, the calorimetrically obtained onset and completion curves on PyrPC/DPPC MLVs (Somerharju et al., 1985) are in reasonable agreement with the solidus and liquidus curves determined by our method (see Table I).

Preliminary experiments in which E/M vs. temperature plots for PyrPC/DEPC, PyrSPM/bovine brain sphingomyelin, PyrSPM/C_{16}SPM,PyrSPM/C_{18}SPM mixtures were determined (all N-shaped) indicate that the pyrene-labeled lipids mix nonideally with the natural phospholipid component in the phase transition region. These results, which will be presented in a later paper, suggest that pyrene lipids in general do not mimic any particular phospholipid; however, the PyrPC/DPPC and the PyrPC/DMPC experiments show that pyrene lipids may mix less ideally with some lipids than with others. Since the shape of an E/M vs. temperature plot for PyrSPM in DMPC is very similar to that of the PyrPC/DMPC plot, this difference in mixing may result from the fact that certain matrix lipids such as DMPC can accommodate the pyrene moiety better than others as opposed to the pyrene lipid mimicking the physical behavior of a particular lipid. However, an E/M vs. temperature plot for a 2% PyrSPM/8% C_{16}SPM/90% POPC mixture suggests that PyrSPM monitors the C_{16}SPM environment below the sphingomyelin T_m and not the bulk POPC lipid (data not shown). Therefore, although pyrene lipid mimic the class of lipid to which they below, they nevertheless are unique molecules. The degree to which they mimic a specific nonfluorescent phospholipid molecule can only be assessed by a study of the thermodynamics of mixing of the two molecules in a bilayer.

ACKNOWLEDGMENTS

We thank Dr. Michael L. Johnson and Martin Straume for their technical assistance with the computer analysis, Dr. Frances A. Stephenson for drawing the graphics, and Dr. Thomas C. Markello for his advice and assistance with some of the fluorescence studies.

APPENDIX

(I) (A) Pyrene Rate Parameter Determination

Closed Form. Birks et al. (1963) developed the following method for estimating the rate parameters $k_{DM}C$, k_{MD}, k_D, and k_M from phase and modulation data. To simplify the analysis, $k_M = k_{fM} + k_{iM}$, $k_D = k_{fD} + k_{iD}$, $X = k_M + k_{DM}C$, and $Y = k_D + k_{MD}$.

The monomer and excimer fluorescence intensities are described by the expressions:

$$i_M(t) = [k_{fM}(\lambda_2 - X)/(\lambda_2 - \lambda_1)](e^{-\lambda_1 t} + Ae^{-\lambda_2 t}) \quad (6)$$

$$i_D(t) = [k_{fD}k_{DM}C/(\lambda_2 - \lambda_1)](e^{-\lambda_1 t} - e^{-\lambda_2 t}) \quad (7)$$

where $i_M(t)$ and $i_D(t)$ are the monomer and excimer fluorescence intensities, respectively.

$$\lambda_{1,2} = (1/2)[X + Y \mp [(Y - X)^2 + 4k_{DM}k_{MD}C]^{1/2}] \quad (8)$$

and

$$A = (X - \lambda_1)/(\lambda_2 - X) \quad (9)$$

If λ_1, λ_2, A, and k_M are known, then $k_{DM}C$, k_{MD}, and k_D can be determined by solving the following equations successively (Birks et al., 1964):

$$X = (A\lambda_2 + \lambda_1)/(A + 1) \quad (10)$$

$$k_{DM}C = X - k_M \quad (11)$$

$$Y = \lambda_1 + \lambda_2 - X \quad (12)$$

$$k_{MD} = (X - \lambda_1)(\lambda_2 - X)/(k_{DM}C) \quad (13)$$

$$k_D = Y - k_{MD} \quad (14)$$

If the concentration is known, then

$$k_{DM} = k_{DM}C/C \quad (15)$$

k_M is simply the inverse of the monomer lifetime at infinite dilution ($C = 0$). When the monomer lifetime is measured as a function of concentration, k_M can be estimated by extrapolating to zero probe concentration using a third-order polynomial fit. Modulation lifetimes are used to estimate k_M since phase lifetimes are sensitive to small errors in the phase shifts at longer lifetimes (Spencer, 1970).

λ_1, λ_2, and A can be determined from the excimer and monomer modulation ratios (m_D and m_M, respectively) and the excimer phase shift (ϕ_D). The complete theory has been published previously (Birks et al., 1963), but briefly λ_1 and λ_2 are determined from the excimer lifetime parameters ϕ_D and m_D in the following manner:

$$\phi_D = \phi_1 + \phi_2 \quad (16)$$

$$m_D = \cos\phi_1 \cos\phi_2 \quad (17)$$

where

$$\phi_1 = \tan^{-1}(\omega/\lambda_1) \quad (18)$$

$$\phi_2 = \tan^{-1}(\omega/\lambda_2) \quad (19)$$

and ω is the angular frequency of the modulation. Solving eq 16 and 17 simultaneously results in

$$\phi_1 = (1/2)[\phi_D + \cos^{-1}(2m_D - \cos\phi_D)] \quad (20)$$

and

$$\phi_2 = \phi_D - \phi_1 \quad (21)$$

Then ϕ_1 and ϕ_2 are substituted into eq 18 and 19 to obtain λ_1 and λ_2.

The last unknown, parameter A, is determined by solving the quadratic equation:

$$A^2\lambda_1^2(m_2^2 - m_M^2) + 2A\lambda_1\lambda_2[m_1m_2\cos(\phi_2 - \phi_1) - m_M^2] + \lambda_2^2(m_1^2 - m_M^2) = 0 \quad (22)$$

where $m_1 = \cos\phi_1$, and $m_2 = \cos\phi_2$.

Birks' analysis must be slightly modified since the computed rate parameters k_D, k_{DM}, and k_{MD} were found to be dependent on the probe concentration which is not predicted in theory. The above result was observed for all lipid systems tested as well as for pyrene in ethanol. It is possible that ϕ_D, which is greater than 90°, cannot be measured accurately at 6 MHz (Barrow & Lentz, 1983). ϕ_M is generally less than 70° and can be determined reliably at 6 MHz. A ϕ_D can be calculated from m_D, m_M, and ϕ_M by using the expression:

$$(\phi_D)_{calcd} = \phi_M + \tan^{-1}[(m_M/m_D)^2 - 1] \quad (23)$$

Equation 23 was derived from eq 4 and 26 and recalling that

$\tau_D = 1/Y$. When $(\phi_D)_{calcd}$, m_D, and m_M are substituted into Birks' analysis, the calculated rate parameters are concentration independent as the theory predicts.

Iterative Method. Since $(\phi_D)_{calcd}$, m_M, and m_D are not completely independent parameters, it is important to compare the computed rate parameters with those calculated by using an independent analysis which utilizes ϕ_M, m_M, and m_D directly. The following equations (Lakowicz and Balter, 1982) may be used to calculate the three rate parameters:

$$\phi_M = \tan^{-1}\left[\frac{\omega(\alpha Y - \beta + \omega^2)}{\alpha\omega^2 + (\beta - \omega^2)Y}\right] \quad (24)$$

$$m_M = \frac{\beta}{Y}\left[\frac{Y^2 + \omega^2}{(\beta - \omega^2)^2 + \alpha^2\omega^2}\right]^{1/2} \quad (25)$$

$$m_D = m_M\frac{Y}{(Y^2 + \omega^2)^{1/2}} \quad (26)$$

where

$$\alpha = k_M + k_D + k_{DM}C + k_{MD}$$

$$\beta = k_Mk_D + k_Dk_{DM}C + k_Mk_{MD}$$

Again k_M can be estimated from the monomer modulation lifetime data. The three unknowns can be solved by using a nonlinear least-squares curve fitting program, which is a modification of the Gauss–Newton procedure (Johnson et al., 1981). The three equations are used as functions to which initial guesses of k_D, $k_{DM}C$, and k_{MD} are fit. At each specific concentration, ϕ_M, m_M, and m_D are entered as the experimental observables. k_M is considered a constant. From the initial guesses of the three rate parameters, ϕ_M, m_M, and m_D are calculated by using eq 24–26. The algorithm finds a better guess for k_D, $k_{DM}C$, and k_{MD} such that the sum of the squares of the residuals, the differences between $(\phi_M, m_M, m_D)_{calcd}$ and $(\phi_M, m_M, m_D)_{exptl}$, is a minimum. This iterative process is terminated when k_D, $k_{DM}C$, and k_{MD} fail to change within a specified tolerance limit.

The two methods were tested for PyrPC in POPC, and the mean estimates of k_D, $k_{DM}C$, and k_{MD} agreed to within 1%. Both analyses have advantages. Birks' analysis is a convenient closed form analysis, while the nonlinear least-squares method utilizes three independent experimental observables directly. Either method may be used since the calculated rate parameters from both analyses are in good agreement.

(B) C_f and C_g Determination

In accordance with the result of Forster and Kasper (1955), rate parameters that are connected with the association and dissociation of monomers and dimers, respectively, will depend on the surrounding viscosity and therefore will have different values in gel and liquid-crystalline phases. Since k_{fM} is viscosity independent and describes an intrinsic property of the fluorophore, it is assumed that $k_{fM}^g = k_{fM}^f = k_{fM}$.

Definitions. We define

$$C_T = M/(M + L)$$

where M = total number of pyrene molecules, L = total number of phospholipid molecules, and C_T = total molar ratio and

$$\sigma_M = M_f/M \qquad \sigma = \frac{M_f + L_f}{M_f + M_g + L_f + L_g}$$

$$C_f = M_f/(M_f + L_f) \qquad C_g = M_g/(M_g + L_g)$$

where M_f = number of pyrene in fluid phase, L_f = number of lipid in fluid phase, M_g = number of pyrene in gel phase, and L_g = number of lipid in gel phase. Using these equations and the lever rule

$$\sigma_M = M_f/(M_f + M_g) = \frac{M_f}{M_f + L_f}\frac{M_f + L_f}{M_f + M_g + L_f + L_g}\frac{M_f + M_g + L_f + L_g}{M_f + M_g} = C_f\sigma\frac{1}{C_T} = C_f\frac{C_T - C_g}{C_f - C_g}\frac{1}{C_T}$$

Initial Conditions. The excitation rate of the monomers is independent of the phase; therefore

$$M_g^*(0)/M_f^*(0) = M_g/M_f \qquad D_g^*(0) = D_f^*(0) = 0$$

where the asterisk represents an excited molecule, D is the number of excimer, and (0) denotes time $t = 0$.

The equations relating E/M and ϕ_M to C_f and C_g are obtained by modifying the original derivation of Birks et al. (1963) to take into account two phases.

(C) E/M Derivation

The E/M derivation is

$$i_M(t) = k_{fM}\left[\frac{M_g^*(t) + M_f^*(t)}{M_g^*(0) + M_f^*(0)}\right] = k_{fM}\left\{\frac{M_g^*(0)}{M_g^*(0) + M_f^*(0)}\left[\frac{\lambda_2^g - X^g}{\lambda_2^g - \lambda_1^g}e^{-\lambda_1^g t} + \frac{X^g - \lambda_1^g}{\lambda_2^g - \lambda_1^g}e^{-\lambda_2^g t}\right] + \frac{M_f^*(0)}{M_g^*(0) + M_f^*(0)}\left[\frac{\lambda_2^f - X^f}{\lambda_2^f - \lambda_1^f}e^{-\lambda_1^f t} + \frac{X^f - \lambda_1^f}{\lambda_2^f - \lambda_1^f}e^{-\lambda_2^f t}\right]\right\} = k_{fM}[g_1e^{-\lambda_1^g t} + g_2e^{-\lambda_2^g t} + \delta_1e^{-\lambda_1^f t} + \delta_2e^{-\lambda_2^f t}] \quad (27)$$

where eq 6 and 7 were used from the paper of Birks et al. (1963) and

$$g_1 = (1 - \sigma_M)\left(\frac{\lambda_2^g - X^g}{\lambda_2^g - \lambda_1^g}\right) \qquad \delta_1 = \sigma_M\left(\frac{\lambda_2^f - X^f}{\lambda_2^f - \lambda_1^f}\right)$$

$$g_2 = (1 - \sigma_M)\left(\frac{X^g - \lambda_1^g}{\lambda_2^g - \lambda_1^g}\right) \qquad \delta_2 = \sigma_M\left(\frac{X^f - \lambda_1^f}{\lambda_2^f - \lambda_1^f}\right)$$

$$i_D(t) = \frac{k_{fD}^gD_g^*(t) + k_{fD}^fD_f^*(t)}{M_g^*(0) + M_f^*(0)} = \frac{M_g^*(0)}{M_g^*(0) + M_f^*(0)}\frac{k_{fD}^gk_{DM}^gC_g}{\lambda_2^g - \lambda_1^g}(e^{-\lambda_1^g t} - e^{-\lambda_2^g t}) + \frac{M_f^*(0)}{M_g^*(0) + M_f^*(0)}\frac{k_{fD}^fk_{DM}^fC_f}{\lambda_2^f - \lambda_1^f}(e^{-\lambda_1^f t} - e^{-\lambda_2^f t}) = (1 - \sigma_M)\frac{k_{fD}^gk_{DM}^gC_g}{\lambda_2^g - \lambda_1^g}(e^{-\lambda_1^g t} - e^{-\lambda_2^g t}) + \sigma_M\frac{k_{fD}^fk_{DM}^fC_f}{\lambda_2^f - \lambda_1^f}(e^{-\lambda_1^f t} - e^{-\lambda_2^f t}) \quad (28)$$

where eq 8 was used from the paper of Birks et al. (1963). The total quantum yield of monomer fluorescence is

$$I_M = \int_0^\infty i_M(t)\,dt = k_{fM}(g_1/\lambda_1^g + g_2/\lambda_2^g + \delta_1/\lambda_1^f + \delta_2/\lambda_2^f) \quad (29)$$

The total quantum yield of excimer fluorescence is

$$I_D = \int_0^\infty i_D(t)\,dt = (1 - \sigma_M)\frac{k_{fD}{}^g k_{DM}{}^g C_g}{\lambda_1{}^g \lambda_2{}^g} + \sigma_M \frac{k_{fD}{}^f k_{DM}{}^f C_f}{\lambda_2{}^f \lambda_1{}^f} \quad (30)$$

Therefore

$$E/M = \left[(1 - \sigma_M)\frac{k_{DM}{}^g C_g k_{fD}{}^g}{\lambda_1{}^g \lambda_2{}^g k_{fM}} + \sigma_M \frac{k_{DM}{}^f C_f k_{fD}{}^f}{\lambda_1{}^f \lambda_2{}^f k_{fM}} \right] \Big/ [g_1/\lambda_1{}^g + g_2/\lambda_2{}^g + \delta_1/\lambda_1{}^f + \delta_2/\lambda_2{}^f] \quad (2)$$

(D) ϕ_M Determination

From Birks et al. (1963), the monomer fluorescence response, $f(t)$, is given by

$$f_M(t) = \int_{-\infty}^{t} C_o(1 + m_p e^{i\omega t'}) i_M(t - t')\,dt' \quad (31)$$

where $C_o(1 + m_p e^{i\omega t'})$ is the exciting light function and

$$i_M(t) = k_{fM}[g_1 e^{-\lambda_1{}^g t} + g_2 e^{-\lambda_2{}^g t} + \delta_1 e^{-\lambda_1{}^f t} + \delta_2 e^{-\lambda_2{}^f t}]$$

After integration of eq 31

$$f_M(t) = C_o k_{fM}\left[\frac{g_1}{\lambda_1{}^g} + \frac{g_2}{\lambda_2{}^g} + \frac{\delta_1}{\lambda_1{}^f} + \frac{\delta_2}{\lambda_2{}^f} \right] \times \left\{ 1 + m_p \left[\left(\frac{g_1}{\lambda_1{}^g + i\omega} + \frac{g_2}{\lambda_2{}^g + i\omega} + \frac{\delta_1}{\lambda_1{}^f + i\omega} + \frac{\delta_2}{\lambda_2{}^f + i\omega} \right) \Big/ \left(\frac{g_1}{\lambda_1{}^g} + \frac{g_2}{\lambda_2{}^g} + \frac{\delta_1}{\lambda_1{}^f} + \frac{\delta_2}{\lambda_2{}^f} \right) \right] e^{i\omega t} \right\} \quad (32)$$

from where the angle of modulation (ϕ_M)

$$\phi_M = \tan^{-1}\left[\omega \left[\frac{g_1}{(\lambda_1{}^g)^2 + \omega^2} + \frac{g_2}{(\lambda_2{}^g)^2 + \omega^2} + \frac{\delta_1}{(\lambda_1{}^f)^2 + \omega^2} + \frac{\delta_2}{(\lambda_2{}^f)^2 + \omega^2} \right] \Big/ \left[\frac{g_1 \lambda_1{}^g}{(\lambda_1{}^g)^2 + \omega^2} + \frac{g_2 \lambda_2{}^g}{(\lambda_2{}^g)^2 + \omega^2} + \frac{\delta_1 \lambda_1{}^f}{(\lambda_1{}^f)^2 + \omega^2} + \frac{\delta_2 \lambda_2{}^f}{(\lambda_2{}^f)^2 + \omega^2} \right] \right] \quad (3)$$

(II) The pyrene fluorescence rate parameters are generally not determined in phospholipid bilayer studies. Many of the assumptions used in pyrene fluorescence experiments in fluid membranes are based on organic solvent studies and therefore can be tested by determining the rate parameters in fluid bilayers.

We have shown the pyrene fluorescence rate parameters in fluid bilayers to have the following characteristics. The rate of excimer formation ($k_{DM}C$) increases linearly with temperature for all three lipid mixtures. In all three PyrPC/PC systems, the rate of excimer dissociation, k_{MD}, is relatively low in the fluid phase, and since the lifetime of the excimer (τ_D) is inversely proportional to the sum of the k_D and k_{MD} (Lakowicz & Balter, 1982), the temperature dependence of τ_D is dominated by the temperature dependence of k_D. The same relationship is observed for pyrene in cyclohexane (Birks et al., 1963) and later assumed to be the case in fluid bilayers (Galla & Sackmann, 1974). The shape of $k_{DM}C\tau_D$ vs. temperature plots for liquid-crystalline systems are almost identical with both the corresponding E/M and $k_{DM}C$ plots (data not shown). This result indicates that the temperature dependence of τ_D has only a minor effect on the shape of an E/M vs. temperature plot for a fluid system. Since the probe is randomly distributed in the liquid-crystalline state, the shape of the E/M vs. temperature curve is due to the temperature dependence of k_{DM}. Birks et al. (1963) determined the fluorescence rate parameters for pyrene in cyclohexane and showed that excimer formation is a diffusion-controlled process in organic solvents. Since the pyrene rate parameters calculated for fluid bilayers using the method of Birks et al. (1963) are in reasonable agreement with the results obtained for pyrene in cyclohexane, this suggests that excimer formation is probably diffusion controlled in fluid bilayers as proposed by Galla and Sackmann (1974).

Very little information is available concerning pyrene fluorescence in gel bilayers. Excimer formation is almost certainly not controlled by lateral diffusion under these circumstances since the lateral diffusion coefficient of fluorescent lipid analogues is known to be several orders of magnitude smaller in the gel phase than in the liquid-crystalline phase by photobleach recovery methods (Wu et al., 1977; Smith & McConnell, 1978; Fahey & Webb, 1978). The rate of excimer formation, $k_{DM}C$, for PyrPC in DPPC is, however, 6-fold larger in the gel than in the fluid phase and is about 2-fold larger for PyrPC in DMPC. Since in the gel phase, lateral diffusion is essentially zero, the rate of excimer formation must be controlled by small intramolecular movements of the fluorophore that increase pyrene ring overlaps and decrease inter-ring distances of essentially stationary molecules. It is also possible that the local effective concentration of pyrene moieties is larger in the gel phase than in the fluid state because in the gel state all of the pyrene moieties are located at about the same depth in the bilayer since the methylene chains are essentially in an all-trans configuration. This is in contrast to the situation in the liquid-crystalline state where the large number of gauche conformations seem to distribute pyrene moieties at different depths in the bilayer. Therefore, the local pyrene concentration will be effectively larger in the gel phase that in the fluid phase in the time frame of the measurement.

The difference in k_{DM} between PyrPC/DPPC and PyrPC/DMPC gel phases may be explained as follows. 10-(1-Pyrenyl)decanoic acid and palmitic acid are approximately equivalent in chain length while myristic acid is two carbons shorter. In the gel state PyrPC and DPPC molecules extend to the same depth in the bilayer, and therefore, the rate of excimer formation in a given monolayer is proportional to the local probe concentration in that monolayer. In comparison, PyrPC and DMPC molecules may interdigitate in the gel phase which may lead to PyrPC molecules from one monolayer sterically hindering the rate of excimer formation in the adjacent monolayer. As a result, k_{DM} will be smaller in PyrPC in DMPC relative to PyrPC in DPPC in the gel phase.

The lifetime of the excimer (τ_D) in the gel phase is about half the value in the fluid phase of both systems. This result is contrary to previously reported lifetime studies when different fluorescent probes such as DPH or parinaric acid are used (Parasassi et al., 1984; Sklar et al., 1977). These studies indicate that the lifetime is longer in the gel state. The excimer lifetime is the inverse of the sum of k_D and k_{MD} (Lakowicz & Balter, 1982). τ_D in fluid bilayers is dominated by the temperature dependence of k_D, but in the gel phase a high rate of excimer dissociation, k_{MD}, is responsible for shortening the excimer lifetime. The reason for excimer instability in the gel state is not known.

Registry No. DPPC, 2644-64-6; DMPC, 13699-48-4; POPC, 6753-55-5; PyrPC, 70700-33-3.

REFERENCES

Barenholz, Y., Gibbes, D., Litman, B. J., Goll, J., & Thompson, T. E. (1977) *Biochemistry 16*, 2806–2810.

Barrow, D. A., & Lentz, B. R. (1983) *J. Biochem. Biophys. Methods 7*, 217–234.
Birks, J. B., Dyson, D. J., & Munro, I. H. (1963) *Proc. R. Soc. London, Ser. A 275*, 575–588 (part II).
Birks, J. B., Dyson, D. J., & King, T. A. (1964) *Proc. R. Soc. London, Ser. A 277*, 270–278 (part III).
Chong, P. L.-G., & Thompson, T. E. (1985) *Biophys. J. 47*, 613–621.
Correa-Freire, M. C., Barenholz, Y., & Thompson, T. E. (1982) *Biochemistry 21*, 1244–1248.
Fahey, P. F., & Webb, W. W. (1978) *Biochemistry 17*, 3046–3053.
Forster, Th., & Kasper, K. (1955) *Z. Elektrochem. 59*, 976–980.
Frank, A., Barenholz, Y., Lichtenberg, D., & Thompson, T. E. (1983) *Biochemistry 22*, 5647–5651.
Freire, E., Markello, T., Rigell, C., & Holloway, P. W. (1983) *Biochemistry 22*, 1675–1680.
Galla, H.-J., & Sackmann, E. (1974) *Biochim. Biophys. Acta 339*, 103–115.
Galla, H.-J., & Sackmann, E. (1975) *J. Am. Chem. Soc. 97*, 4114–4120.
Galla, H.-J., Hartmann, W., Theilen, U., & Sackmann, E. (1979) *J. Membr. Biol. 48*, 215–236.
Hresko, R. C., Markello, T. C., Barenholz, Y., & Thompson, T. E. (1985) *Chem. Phys. Lipids 38*, 263–273.
Hubbell, W. L., & McConnell, H. M. (1971) *J. Am. Chem. Soc. 93*, 314–326.
Johnson, M. L., Correia, J. J., Yphantis, D. A., & Halvorson, H. R. (1981) *Biophys. J. 36*, 575–588.
Lakowicz, J. R., & Balter, A. (1982) *Biophys. Chem. 16*, 99–115.
Lakowicz, J. R., Cherek, H., & Balter, A. (1981) *J. Biochem. Biophys. Methods 5*, 131–146.
Lee, A. G. (1977) *Biochim. Biophys. Acta 472*, 285–344.
Mabrey, S., & Sturtevant, J. M. (1976) *Proc. Natl. Acad. Sci. U.S.A. 73*, 3862–3866.
Mason, J. T., Broccoli, A. V., & Huang, C. (1981) *Anal. Biochem. 113*, 96–101.
Massey, J. B., Gotto, A. M., & Pownall, H. J. (1982) *Biochemistry 21*, 3630–3636.
Massey, J. B., Hickson, D., She, H. S., Sparrow, J. T., Via, D. P., Gotto, A. M., & Pownall, H. J. (1984) *Biochim. Biophys. Acta 794*, 274–280.
McElhaney, R. N. (1982) *Chem. Phys. Lipids 30*, 229–259.
Parasassi, T., Conti, F., Glaser, M., & Gratton, E. (1984) *J. Biol. Chem. 259*, 14011–14017.
Pownall, H. J., Hickson, D., Gotto, A. M., & Massey, J. B. (1982) *Biochim. Biophys. Acta 712*, 169–176.
Roseman, M. A., & Thompson, T. E. (1980) *Biochemistry 19*, 439–444.
Seelig, A., & Seelig, J. (1974) *Biochemistry 13*, 4839–4845.
Silvius, J. R. (1982) in *Lipid-Protein Interactions* (Jost, P., & Griffith, O. M., Eds.) Vol. 2, pp 239–281, Wiley, New York.
Sklar, L. A., Hudson, B. S., & Simoni, R. D. (1977) *Biochemistry 16*, 819–828.
Smith, B. A., & McConnell, H. M. (1978) *Proc. Natl. Acad. Sci. U.S.A. 75*, 2759–2763.
Somerharju, P. J., Virtanen, J. A., Edlund, K. K., Vainio, P., & Kinnunen, P. K. J. (1985) *Biochemistry 24*, 2773–2781.
Spencer, R. D. (1970) Ph.D. Thesis, University of Illinois at Urbana–Champaign.
Sugár, I. P., & Monticelli, G. (1985) *Biophys. J. 48*, 283–288.
Usher, J. R., Epand, R. M., & Papahadjopoulos, D. (1978) *Chem. Phys. Lipids 22*, 245–253.
Vanderkooi, J. M., & Callis, J. B. (1974) *Biochemistry 13*, 4000–4006.
Wiener, J. R., Pal, R., Barenholz, Y., & Wagner, R. R. (1985) *Biochemistry 24*, 7651–7658.
Wong, M., Brown, R. E., Barenholz, Y., & Thompson, T. E. (1984) *Biochemistry 23*, 6498–6505.
Wu, E.-S., Jacobson, K., & Papahadjopoulos, D. (1977) *Biochemistry 16*, 3936–3941.